Effects of post-translational modifications on prion protein aggregation and the propagation of scrapie-like characteristics in vitro

Available online at www.sciencedirect.com
ScienceDirect
Biochimica et Biophysica Acta 1774 (2007) 792–802
Biochimica et Biophysica Acta
BBA
www.elsevier.com/locate/bbapap

Effects of post-translational modifications on prion protein aggregation and the propagation of scrapie-like characteristics in vitro

Denise V. Dear [a,*], Duncan S. Young [a], Jurate Kazlauskaite [b], Filip Meersman [c], David Oxley [e], Judith Webster [e], Teresa J.T. Pinheiro [b], Andrew C. Gill [d], Igor Bronstein [d], Christopher R. Lowe [a]

[a] Institute of Biotechnology, University of Cambridge, Tennis Court Road, Cambridge, CB2 1QT, UK
[b] Department of Biological Sciences, Gibbet Hill Campus, University of Warwick, Coventry, CV4 7AL, UK
[c] Department of Chemistry, University of Cambridge, Lensfield Road, Cambridge, CB2 1EW, UK
[d] Institute for Animal Health, Compton, Newbury, Berkshire, RG20 7NN, UK
[e] Proteomics Research Group, Babraham Institute, Babraham, Cambridge, CB2 4AT, UK

Received 17 September 2006; received in revised form 26 April 2007; accepted 7 May 2007
Available online 18 May 2007

Abstract

Prion diseases, or transmissible spongiform encephalopathies (TSEs) are typically characterised by CNS accumulation of PrP^{Sc}, an aberrant conformer of a normal cellular protein PrP^{C}. It is thought PrP^{Sc} is itself infectious and the causative agent of such diseases. To date, no chemical modifications of PrP^{Sc}, or a sub-population thereof, have been reported. In this study we have investigated whether chemical modification of amino acids within PrP might cause this protein to exhibit aberrant properties and whether these properties can be propagated onto unmodified prion protein. Of particular interest were post-translational modifications resulting from physiological conditions shown to be associated with TSE disease. Here we report that in vitro exposure of recombinant PrP to conditions that imitate the end effects of oxidative/nitrative stress in TSE-infected mouse brains cause the protein to adopt many of the physical characteristics of PrP^{Sc}. Most interestingly, these properties could be propagated onto unmodified PrP protein when the modified protein was used as a template. These data suggest that post-translational modifications of PrP might contribute to the initiation and/or propagation of prion protein-associated plaques in vivo during prion disease, thereby high-lighting novel biochemical pathways as possible therapeutic targets for these conditions.

Keywords: Prion protein; Aggregation; Post-translational modification; Nitro-tyrosine; Oxidative and nitrative stress

1. Introduction

The transmissible spongiform encephalopathies include bovine spongiform encephalopathy (BSE) in cattle [1], Creutzfeldt–Jakob disease (CJD) in humans [2] and scrapie in sheep [3]. Also known as prion diseases, they are fatal transmissible neurodegenerative conditions of the central nervous system (CNS) which are characterised by the accumulation of PrP^{Sc} [4] an abnormal isomer of the host protein PrP^{C}. It has been hypothesized that the transmissible agent of these diseases consists solely of proteinaceous material [5]. Consequently, it is proposed that PrP^{Sc} forms part, or all, of the infectious prion agent and is responsible for the modification of PrP^{C}. The physical characteristics of PrP^{Sc} are profoundly different to those of PrP^{C} [5]. PrP^{Sc} occurs as an insoluble aggregate which is often amyloid in character, with an increased β-sheet secondary structure. It is partially resistant to proteinase K treatment and can act as a template for the conversion of PrP^{C} to PrP^{Sc}.

Abbreviations: CNS, central nervous system; PrP^{Sc}, disease-associated isoform of prion protein; PrP^{C}, normal cellular isoform of PrP; TSE, transmissible spongiform encephalopathy; rPrP, recombinant full-length alpha-helical prion protein; MPO, myeloperoxidase; HPLC, high pressure liquid chromatography; FT-IR, Fourier transform infra-red spectroscopy; LC-MS/MS, liquid chromatography tandem mass spectrometry; ThT, thioflavine T; PK, proteinase K; PMSF, phenymethyl sulphonyl fluoride; NT, nitrotyrosine; MNP, myeloperoxidase, nitrite and peroxide reactants; NMR, nuclear magnetic resonance; SAFs, scrapie-associated fibrils; CJD, Creutzfeldt–Jakob Disease; PTM, post-translational modification

* Corresponding author. Tel.: +44 1223 334158; fax: +44 1223 334162.
E-mail address: happyprion@aol.com (D.V. Dear).

1570-9639/$ - see front matter © 2007 Elsevier B.V. All rights reserved.
doi:10.1016/j.bbapap.2007.05.005

Attempts to validate the protein-only hypothesis have focussed on converting recombinant protein into a form that resembles PrP^{Sc} displaying both proteinase resistance and infectivity. Early work produced proteinase K resistant recombinant PrP but there was no demonstrated infectivity [6]. However, more recent attempts have demonstrated evidence of infectivity of an N-terminally truncated recombinant protein refolded into a beta-sheet rich conformation [7,8] which fibrillized readily. Other studies have produced oligomeric forms of recombinant PrP, which possess other characteristics of PrP^{Sc} but appear not to be infectious [9,10]. Within recent work, there have been a few reports regarding the chemical modifications of prion protein each of which indicates varying degrees of success in changing the protein's conformation [11–16].

Although the original studies on PrP^{Sc} maintain that there is no difference in PrP^{C} and PrP^{Sc} primary structure [17], studies of PrP^{Sc} and infectivity titres have suggested that there may be 10^5 molecules of PrP^{Sc} per infectious unit with the possibility that a sub-population of modified protein could be present. Additionally, in long-lived post-mitotic cells such as neurons, macromolecules can accumulate damage in the form of modified amino-acids [18]. Such damage can manifest itself as a progressive change in protein structure, charge and loss of biochemical function. No comprehensive study exists regarding any possible damage to prion protein and its possible significance in the initial formation of PrP^{Sc}. Indeed, given the extended incubation periods and late-stage onset associated with TSE diseases, age-related modifications could realistically have a role in disease progression.

Accordingly, we have been interested in determining to what extent, if any, chemical modification of the prion protein might cause the normal protein to exhibit any properties associated with PrP^{Sc}. We were particularly interested in conditions that might mimic altered physiological states that have been reported to be associated with prion disease. Such a condition is oxidative/nitrative stress, which has been reported to be present in the brains of scrapie-infected mice [19,20]. More recently, protein deposition in the form of disease-associated PrP^{Sc} has been shown to correlate with the presence of oxidative stress in TSE disease [21]. Oxidative stress can be defined as the conditions under which oxidative free radicals are present in excess of the cellular antioxidant defense mechanisms. This causes a destructive condition since reactive oxygen and/or nitrogen species, such as superoxide, peroxynitrite and hydroxyl radicals, modify cellular components resulting in lipid peroxidation, nitration and/or cross-linking of proteins and nucleic acid mutations. This results in a fingerprint of characteristic oxidative stress markers such as nitrotyrosine groups and/or dityrosine cross-links being present in proteins of the target tissue [22]. It is apparent that a number of neurodegenerative diseases exhibit characteristic protein aggregation accompanied by tyrosine nitration in the presence of oxidative stress reactants which may include an oxidative enzyme [23,24]. For example, rapid aggregation of α-synuclein, a protein identified in the aggregates known as Lewy bodies associated with Parkinson's disease, can be achieved in vitro by exposure to nitrative and oxidative agents associated with oxidative stress [25].

Since oxidant-producing inflammatory enzyme systems have been associated with other neurodegenerative diseases [26], we decided to use such an oxidant system in this study to achieve the post-translational modifications (PTMs) rather than alternative methods of protein nitration and oxidation [27]. We show that recombinant PrP protein exposed to an oxidant environment exhibits many of the physical characteristics of scrapie-associated prion protein and most importantly, the modified PrP reveals an altered secondary structural content similar to that reported for PrP^{Sc} [17]. In addition, we show that many of these PrP^{Sc}-like properties can be templated onto unmodified protein in vitro. This raises the possibility that such modification of prion protein might have a role in the initiation of PrP^{Sc} formation and contribute to the presence of prion protein-associated plaques in vivo, thereby high-lighting potential routes to novel targets for therapeutic reagents in the future.

2. Methods

2.1. Ovine recombinant PrP

Oxidatively-refolded ovine recombinant PrP (amino acid residues 25–233, with valine at residue 136, arginine at 154 and glutamine at 171; hereafter referred to as rPrP) was provided by the Institute for Animal Health, Compton. Protein was expressed in 1B392 *E. coli* and purified to homogeneity following previously published methodology [28]. Electrospray mass spectrometry of rPrP was used to confirm the correct amino acid sequence for this allelic variant of the ovine prion protein and the presence of an internal disulphide bond. Circular dichroism showed that the protein was predominately α-helical in structure.

2.2. Protein oxidation and nitration

Chemical modification of rPrP or lysozyme (Sigma, UK) was carried out by incubation of the protein (600 μg/ml) with final concentrations of MNP reactants viz. 0.006 U human myeloperoxidase (MPO) (Sigma, UK), 100 mM sodium nitrite and 3% hydrogen peroxide (BDH, UK) at 37 °C with shaking for various periods of time. Residual MPO activity was inhibited by the addition of sodium azide to a final concentration of 25 mM and buffer exchange was carried out into sodium acetate, pH 5.5 using centrifugal concentrators with a 10-kDa cut off (Millipore, UK). For all subsequent investigations apart from mass spectrometry, chemical modification of rPrP or lysozyme (Sigma, UK) was carried out as described previously. For mass spectrometry, concentrations of the reactants were chosen which still allowed for modification of rPrP to be detected on Western blot (see below and p. 11) viz. 0.3% H_20_2 and 10 mM $N0_2$ — but which showed less propensity to aggregation. This was necessary for on-line HPLC-mass spectrometry to be possible. On-line HPLC-mass spectrometry of chemically modified proteins was carried out as described previously [14]. pH was maintained at 5.5 throughout all procedures.

Chemical modification of rPrP was also carried out at four ten-fold dilutions of the above reactants. This was to determine at which dilutions the protein was modified. After incubation at 37 °C with shaking overnight, samples were microfuged to separate aggregating protein as a pellet from that in the supernatant. Pellets were re-dissolved in loading buffer (10 μl) or aliquots (5 μl) of supernatant were mixed with loading buffer (5 μl). These samples were then subjected to SDS-PAGE as described below.

2.3. Fourier-transform infra-red (FTIR) spectroscopy

Attenuated total reflection (ATR) Fourier transform infrared (FT-IR) spectroscopy was used to determine the structural nature of the modified protein. Spectra were recorded at room temperature on a Bruker Vector 22 infrared spectrometer equipped with a liquid nitrogen-cooled mercury cadmium

telluride (MCT) detector at a nominal resolution of 4 cm^{-1}. The spectrometer was continuously purged with dried air to minimize the spectral contribution of atmospheric water. Residual water vapour peaks were subtracted using reference spectra. The internal reflection element was a germanium ATR plate (50×20×2 mm) with an aperture angle of 45° yielding 25 internal reflections. Thin films of hydrated PrP were obtained by depositing 30 μl of sample and evaporating excess water under of N_2 gas. To differentiate between α-helix and random structures, prepared films were subjected to a stream of ^2H_2O-saturated N_2 gas for 30 min at room temperature. Peak fitting of the amide I band (1600–1700 cm^{-1}) was performed on non-deconvoluted spectra using GRAMS 32/AI software (Thermogalactic, USA). Band assignments were made according to Cabiaux et al. [29].

To investigate the structure of templated protein, FTIR spectra were recorded at room temperature on a Bruker Equinox 55 spectrometer equipped with a liquid nitrogen cooled mercury cadmium telluride detector. The sample compartment was continuously purged with dry air. For each sample, 256 interferograms were collected at a spectral resolution of 2 cm^{-1}. Sample and buffer spectra were measured separately and subsequently subtracted using Protein Dynamics software (Bruker). Thin films of hydrated rPrP were obtained by depositing 200 μg of protein in a 30-μl volume on the crystal and subsequent removal of excess water under a gentle N_2 flow.

2.4. Liquid chromatography-tandem mass spectrometry (LC-MS/MS) of modified rPrP

Oxidized/nitrated rPrP was reduced, carbamidomethylated and digested with trypsin (1:100 enzyme:substrate ratio) overnight at 30 °C in 25 mM ammonium bicarbonate at pH 8.5. The peptide products were analysed by on-line LC-MS/MS. The tryptic peptides were separated on a reversed-phase column (0.1×100 mm; Vydac C18) with a gradient of 0–30% (v/v) acetonitrile (containing 0.1% (v/v) formic acid) over 30 min, at a flow rate of 500 nl/min. Peptides were eluted *via* a nanoelectrospray interface into a quadrupole time-of-flight mass spectrometer (Applied Biosystems). The mass spectral data were matched to the protein sequence using Mascot software (Matrix Science) and confirmed by manual interpretation of MS/MS spectra.

2.5. Amyloid formation in aggregated samples

The kinetics of aggregation of chemically modified rPrP samples was monitored in 96-well plates by measurement of optical density (O.D.) at 490 nm at 10 min intervals using a micro-plate reader (Opsys, Jencons, UK). Amyloid formation was detected by one of two methods: aggregated samples were either reacted with Congo Red, applied to glass slides and visualized in polarized light using an Olympus BX41 microscope to show the presence of birefringence [30]; alternatively, addition of 25 μM Thioflavine T (ThT) solution prepared in 50 mM Tris–HCl, pH 8.0 was added to 1 μM modified or unmodified rPrP protein in the wells of a 96-well plate and the mixture incubated for 25 °C for 5 min. Bound ThT was determined by fluorescence measurement (444 nm excitation and 485 nm emission wavelength) at room temperature using a fluorescence plate reader (Thermo Life Sciences, UK). Electron microscopy of aggregated rPrP was performed by negative staining on carbon-coated, 600 mesh, copper grids. Samples were adsorbed to the grids for 30 s, stained for 2 min with 2% (w/v) uranyl acetate and visualized at 100,000 magnification.

2.6. Measurement of proteinase K (PK) sensitivity

Prior to PK treatment, proteins were dialyzed against water using mini dialysis units (Pierce, UK), according to the manufacturer's protocol. Protease resistance was assessed by incubation of protein samples at 37 °C for 1 h with PK (Sigma, UK) at 20 μg/ml. The reaction was stopped by the addition of the protease inhibitor phenylmethylsulphonyl fluoride (PMSF) to a final concentration of 1 mM. Samples were analyzed by SDS-PAGE as described below.

2.7. SDS-PAGE and Western blot analysis of ovine rPrP

In general, protein samples were separated by SDS/PAGE under reducing conditions using pre-cast 4–20% (w/v) tris-glycine gradient gels (Invitrogen, Holland). Bands were visualized using the Coomassie®-based protein stain, SimplyBlue™ (Sigma, UK) according to the manufacturer's protocol. Gels were destained overnight, and then dried at 80 °C for 1 h for storage. The gels displayed in this work are representative of at least 2 experiments. For Western blotting, gels were blotted overnight onto Immobilin-P (Millipore, UK) transfer membranes. Membranes were blocked for 30 min with TBS-T (10 mM Tris/HCl, pH 7.8; 100 mM NaCl and 0.05% Tween 20) containing 5% (w/v) non-fat milk and then incubated with rabbit polyclonal anti-nitrotyrosine (NT) antibody (Cell Signalling Technology, Massachusetts, USA) at 20 °C for 2 h. Binding was detected using biotinylated goat anti-rabbit IgG and visualized using an avidin–peroxidase complex with diaminobenzidine as the substrate (Vector Laboratories, Peterborough, UK). Gel densitometry was carried out using the Scion Image 1.63 software available at http://www.ScionCorp.com.

2.8. Templating procedure

In general, modified rPrP prepared as described above, was mixed at a concentration ratio of approximately 1:100 (modified:unmodified protein) and incubated for 24 h at room temperature with shaking. To ensure that incubated unmodified protein could be distinguished from the modified template, the latter was prepared using concentrations of NO_2^-/H_2O_2 which had been shown by western blot to cause a level of modifications which caused all the modified protein to be pelletted on centrifugation (see Results section below). This was confirmed by analysis of the supernatant by western blot which showed no evidence of protein being present or was below the level of detection of our western blot. After removal of the template samples of the unmodified rPrP remaining in the supernatant were analyzed for PK resistance. This was done by SDS-PAGE analysis followed by Coomassie blue staining and gel densitometry, as described in Methods above.

2.9. Production of radio-labelled rPrP and templating procedure

Radio-labelled rPrP was produced by in vitro transcription/translation as described previously [31]. ^{35}S-labelled translation products were incubated overnight at 37 °C with unlabelled oxidized/nitrated rPrP with shaking. After digestion with PK at 20 μg/ml for 1 h at 37 °C, digests were analyzed by SDS-PAGE.

3. Results

3.1. Characterisation of NO_2^-/H_2O_2 modified rPrP

On exposure of rPrP to a series of dilutions of the MNP (myeloperoxidase, nitrite and peroxide) system, it was found that at high concentrations of nitrite and peroxide, the solution turned yellow and a yellow precipitate was formed. The precipitate was found to be insoluble even in concentrated formic acid. The yellow coloration(λ_{max} ~410 nm, pH 8) was attributed to the presence of nitrotyrosine residues [32,33,25]. Peptidyl nitrotyrosine has been shown previously to produce a yellow coloration (λ_{max} ~428 nm, pH 8) [34,35]. Preliminary experiments were therefore carried out to determine the optimum concentrations of NO_2^-/H_2O_2 that would allow some of the modified protein to remain soluble for subsequent analysis by mass spectrometric methods which tend to require soluble analytes.

Consequently, soluble and pelleted fractions of modified samples were analysed by SDS-PAGE and western blot for the presence of nitrotyrosine. Experiments were carried out to determine the optimum dose range of NO_2^-/H_2O_2 to be used for the modification of rPrP by exposing samples to a dose range of four ten-fold dilutions of the reactants starting at 100 mM

NO_2^-/3% H_2O_2. Soluble and pelleted fractions were analysed by western blot for the presence of nitrotyrosine. At a concentration of 100 mMNO_2^-/3% H_2O_2, nitrotyrosine residues were most abundant in the pelleted fraction of modified rPrP with very little present in the supernatant fraction (Fig. 1). At 10 mMNO_2^-/0.3% H_2O_2, nitrotyrosine was detected in both the pellet and supernatant fractions. At concentrations tested below these ranges viz. 0.1 mM and 1 mM nitrite or 0.03 and 0.003% peroxide, most nitrotyrosine was observed in the supernatant fraction when reactants had been diluted a hundred fold. No nitrotyrosines were detected at the lowest concentrations of reactants used. Routinely, concentrations of NO_2^- in the millimolar range were used to modify rPrP.

In order to identify the nature and extent of amino acid modification following exposure to NO_2^-/H_2O_2, modified rPrP protein was digested with trypsin and the resultant digest was analyzed by LC-MS/MS. Peptides were identified that covered 58% of the sequence and included 10 out of the possible 14 tyrosine residues present in rPrP. The nature and extent of oxidation of specific amino acid residues in rPrP was assessed by difference in molecular mass compared to unmodified residues (Table 1). Cysteine residues are known to be susceptible to oxidation [36] and the cysteine at 217 was completely oxidized to cysteic acid whilst methionine residues were oxidized to sulphoxide and sulphone forms. No data were acquired regarding the cysteine at 182. These oxidations occurred at residues Met132, 137, 157, 209 and 216, and Cys217. The tryptophan residues in the flexible N-terminal region of the protein were also exposed to the oxidative conditions, as amino acid Trp34 and Trp60 converted to the dioxide form. Nitration was confirmed by a mass increase of peptide fragments of 45 Da per modified residue. The highest degree of tyrosine nitration was seen at residues Tyr41 and Tyr52 (60% and 65% modified, respectively). The helix-1 epitope (DY^{148}EDRY^{152}Y^{153}REN) has previously implicated as being susceptible to oxidative modification [37]. Of the tyrosine residues in this region of our modified rPrP, Tyr153 was the most nitrated at ~37%, whilst Tyr148 and Tyr152 were nitrated to a similar extent at approximately 22%.

The C-terminal proximal residues Tyr227 and Tyr228 were also nitrated, but less extensively than those within the N-terminal region. This difference may presumably reflect the fact that the C-terminal residues Tyr227 and Tyr228 are located in the highly structured helix-3 in comparison to those within the unstructured N-terminal region of the protein, which are potentially more solvent exposed and more accessible to modification.

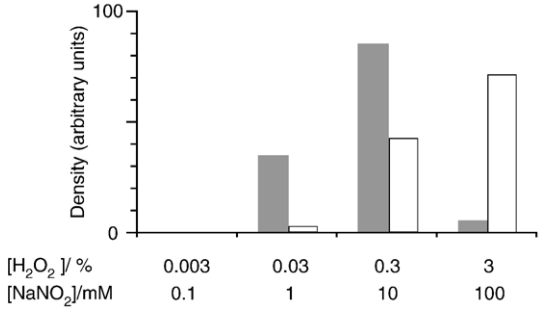

Fig. 1. Dose response of rPrP to NO_2^-/H_2O_2. Recombinant prion protein samples were treated with various concentrations of NO_2^-/H_2O_2 as indicated in Methods. After centrifugation, the pellets were re-dissolved in loading buffer. Equal proportions of the re-dissolved pellets and equal proportions of the supernatants were subjected to SDS-PAGE (see Methods). The modified protein runs as a smear under these conditions, and nitrotyrosine reactivity was therefore quantified by measuring the total optical density in each gel track. No nitrotyrosine reactivity was observed in samples treated with the lowest concentrations of reactants. As the reagent concentration is increased, nitrotyrosine reactivity appears first in the supernatant (grey bars) and then predominantly in the pellet (white bars). At the highest concentration of reactants, nitrotyrosines were confined almost exclusively to the pellet.

Table 1
Mass spectrometric analysis of modified rPrP

Residues	Modifications	Ratio
Cys217	Unmodified:Cysteic acid	0:1
Met132 and Met137	2 sulphone:1 sulphone/1: sulphoxide:2 sulphoxide	0.44:0.77:1
Met157	Sulphone:Sulphoxide	1.3:1
Met209	Sulphone:Sulphoxide	1.54:1
Met216	Sulphone:Sulphoxide	1.2:1
Trp34	Unmodified:Dioxide	0:1
Trp60	Unmodified:Dioxide	0:1
Tyr41	Unmodified:Nitrated	1:1.5
Tyr41 and Tyr52	Unmodified:1 Nitrated:2 Nitrated	1:3.3:2.9
Tyr131	Unmodified:Nitrated	1:0.24
Tyr148	Unmodified:Nitrated	1:0.28
Tyr152	Unmodified:Nitrated	1:0.29
Tyr153	Unmodified:Nitrated	1:0.59
Tyr158	Unmodified:Nitrated	1:0.37
Tyr221	Unmodified:Nitrated	1:0.35
Tyr227 and Tyr228	Unmodified:227-Nitrated: 228-Nitrated:both Nitrated	1:0.66:0.78:0.58

Relative amounts of the different modifications detected at each residue in peptides obtained from modified rPrP. Residue numbering corresponds to native ovine PrP^C. Where two modified residues e.g. Met132 and Met137, Tyr41 and Tyr52, or Tyr227 and Tyr228 occurred in the same peptide fragments and were not resolved by reversed-phase liquid chromatography they were assessed together.

3.2. Biophysical characterisation of modified rPrP aggregates

Preparations of aggregates of modified rPrP were investigated by electron microscopy in order to determine their biophysical characteristics. The majority (>95%) of the modified protein showed larger amorphous structures, some with diameters of up to 50 nm (Fig. 2a). There was also evidence of a fine lattice arrangement of intertwined fibrillar-type material with a diameter of approximately 10 nm (Fig. 2b). Other techniques were also used to examine the nature of the aggregated modified rPrP. Congo red staining showed evidence of some birefringent material indicating the presence of fibrillar structures but this was not confirmed by ThT staining as the amount of fibrillar protein may have been below the sensitivity of the test (data not shown).

FT-IR spectroscopy was used to compare the secondary structure composition of unmodified and modified rPrP protein.

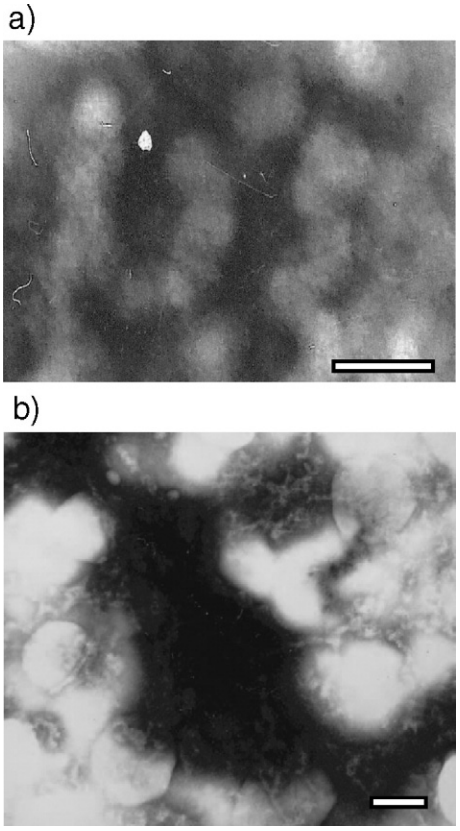

Fig. 2. Electron microscopy of modified rPrP. (a) The majority of the modified protein showed larger amorphous structures. (b) Example of a lattice work of fibrillar-type material present in modified rPrP. Scale bars represent 100 nm.

The modified rPrP protein was prepared as a precipitate under conditions of high concentrations of NO_2^-/H_2O_2 and in the presence of MPO. The FT-IR spectrum of unmodified rPrP contained an amide I band with a maximum absorption at 1652 cm^{-1} characteristic of proteins in a predominantly α-helical conformation (Fig. 3). However, the spectrum of modified rPrP possessed a broader amide I band with maxima at 1648 cm^{-1} and 1621 cm^{-1}, which is more characteristic of β-sheet structure. Peak fitting analysis of the amide I band was employed to quantify the main structural changes of rPrP upon oxidation/nitration. Analysis of the unmodified rPrP amide I band indicated that the protein had a secondary structural content of 48.2% α-helix, 36.4% random coil, 12% β-turns and 3.4% β-sheet. This is in good agreement with NMR structures of recombinant mammalian prion proteins [38,39]. In contrast, modified rPrP had a secondary structure content of 34.7% α-helix, 24% random coil, 15.1% β-turns and 25% β-sheet. This indicated that the major structural change in modified rPrP was an increase in β-sheet and a concomitant decrease in α-helix content, in line with the PrP^C to PrP^{Sc} transition.

3.3. Aggregate formation of modified rPrP

Exposure of rPrP to NO_2^-/H_2O_2 in the presence of MPO resulted in the formation of a yellow precipitate and therefore allowed aggregate formation to be monitored by measuring the turbidity of the reaction mix at 490 nm (Fig. 4a). Turbidity measurements were performed at different concentrations of rPrP to assess the kinetics of oxidation/nitration-induced aggregation of the modified protein (Fig. 4b). The rate of the aggregation reaction was calculated from the gradient of the linear regression of these samples over 0–45 min, and plotted against the respective PrP concentration (Fig. 4c). The increase in optical density was linear over the time monitored and the rate of the reaction was constant over the range measured and the rate of aggregate formation increased linearly with rPrP protein concentration. This confirmed that the reaction rate was first order.

3.4. Modified rPrP displays protease resistance

A characteristic of PrP^{Sc} is its resistance to proteolysis. Accordingly, we investigated whether NO_2^-/H_2O_2 modified rPrP, which had acquired some of the structural features of disease-associated PrP had also acquired resistance to proteolytic degradation. Proteolysis of rPrP by increasing concentration of PK was examined by SDS-PAGE and densitometry. Fig. 5a shows that mature length monomeric unmodified rPrP had a molecular mass of 23 kDa and following treatment with PK at 10 μg/ml was readily digested into polypeptides of apparent molecular mass of 12 and 13 kDa. When higher concentrations of PK were used, smaller peptides of 9 and 5 kDa were observed. Analysis of the profile of production of each of these degradation products indicated that the 12- and 13-kDa products were produced with similar kinetics and subsequently degraded into the 9- and 5-kDa fragments. Most of the unmodified rPrP protein was degraded at PK levels of 100 μg/ml (Fig. 5b). Conversely, modified rPrP was digested in a similar manner to unmodified rPrP but resulted in only a12 kDa fragment which persisted at high concentrations of PK

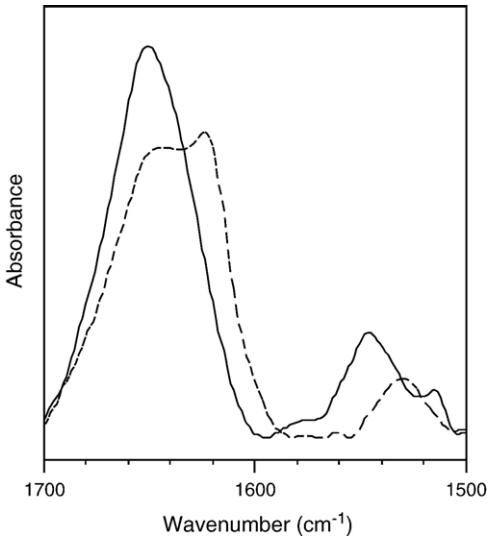

Fig. 3. FTIR spectroscopy of modified rPrP. FT-IR spectroscopic analysis resulted in absorbance spectra for unmodified protein (black line) and modified protein (dashed line). The latter showed a distinct shoulder at 1621 cm^{-1} characteristic of β-sheet structure which was absent in the unmodified protein spectrum. Data shown are representative of three independent experiments.

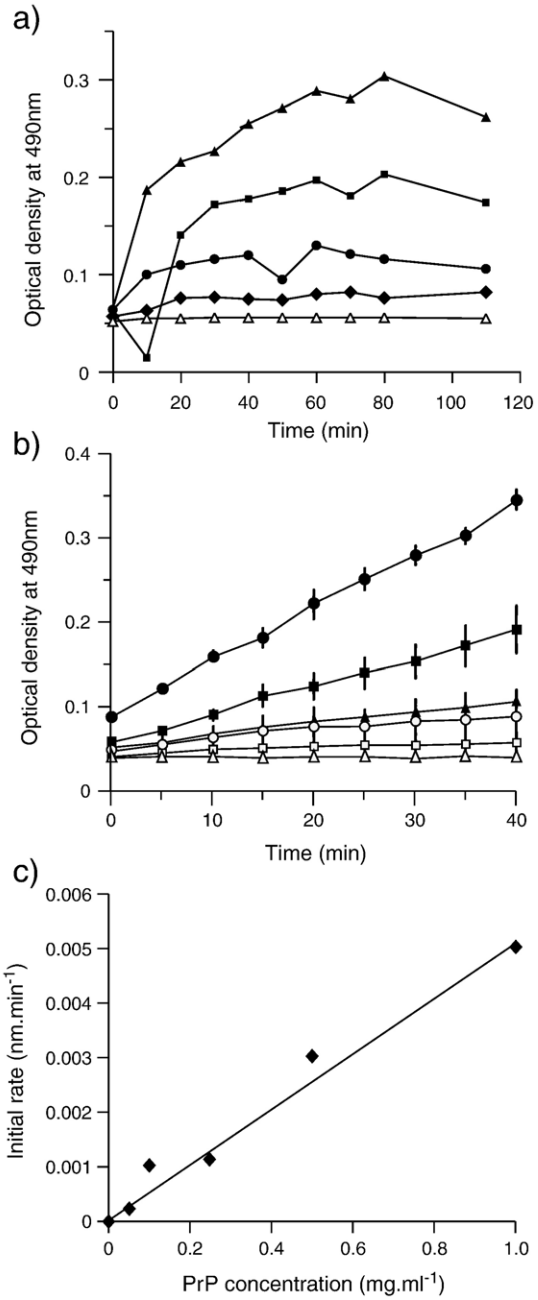

Fig. 4. Aggregation assays of modified rPrP. (a) Aggregation of rPrP monitored in the presence of different combinations of the MNP reactants (concentrations as in Methods), as measured by turbidity at 490 nm. rPrP alone (open triangle) or in the presence of MPO/H_20_2 (closed diamond), MPO/NO_2^- (filled circle), NO_2^-/H_2O_2 (filled square) and NO_2^-/H_2O_2 /MPO (filled triangle). (b) Kinetics of aggregation of rPrP modified in the presence of all MNP reactants (used at ten-fold dilutions of concentrations in Methods) measured by turbidity analysis of different concentrations of rPrP: Filled circle=1 mg/ml, filled square=0.5 mg/ml, filled triangle=0.1 mg/ml, open circle=0.25 mg/ml, open square=0.05 mg/ml and open triangle=−0 mg/ml. The data represents four independent assays, and the error bars correspond to one standard deviation. (c) The rate of the aggregation reaction was calculated as the gradient of the linear regression of these samples over 0–45 min, and plotted against the respective PrP concentration.

(Fig. 5c and d). This suggested that modified rPrP had acquired partial resistance to PK digestion.

3.5. Templating ability of modified rPrP

A striking feature of PrP^{Sc} is its apparent ability to transfer, or template, its structural and PK-resistant properties onto PrP^{C} [40,41]. Accordingly, we investigated whether the NO_2^-/H_2O_2 modified rPrP could induce structural changes and PK resistance in unmodified rPrP. To ensure that unmodified protein which had acquired PK resistance through templating could be distinguished from the modified template, the latter was prepared using concentrations of NO_2^-/H_2O_2 which had been shown previously by western blot to cause a level of modifications which caused all the protein to be pelletted on centrifugation. Samples of modified rPrP were mixed with unmodified rPrP and, subsequently, modified rPrP was removed from the reaction by centrifugation. The structure of templated, unmodified rPrP remaining in the supernatant was assessed by FTIR spectroscopy and compared to the starting, unmodified rPrP. Fig. 6 shows the FT-IR spectrum of unmodified untemplated rPrP, which was characterised by a broad amide I band that lacked any well-resolved secondary structural bands. In contrast, the unmodified templated rPrP is characterised by a maximum at ~1653 cm^{-1} within the amide I band, in addition to a shoulder at ~1620 cm^{-1} typical of β-sheet structures.

We also investigated whether the NO_2^-/H_2O_2 modified rPrP could induce PK resistance in unmodified rPrP. After 24 h incubation, samples of templated rPrP were assessed for acquisition of PK resistance (Fig. 7). Unmodified monomeric rPrP was digested by 10 μg/ml PK with the concomitant appearance of a protein band at 12 kDa, which was subsequently cleaved upon digestion with increased concentration of protease at both 0 and after 24 h incubation (Fig. 7a and c). In contrast, whilst digestion of templated unmodified rPrP with 10 μg/ml PK led to a similar sized 12 kDa fragment at 0 h, after 24 h incubation with the modified template, this fragment was resistant to digestion with up to 100 μg/ml of PK (Fig. 7b and d). The PK resistance profile of templated unmodified rPrP was similar to that seen by modified rPrP. In a further experiment to assess PK resistance of templated rPrP, radiolabelled rPrP translation products were incubated overnight at 37 °C in the presence of unlabelled modified rPrP. After incubation, the reaction mix was subjected to PK digestion followed by SDS-PAGE and autoradiography. Fig. 8 shows that SDS-PAGE analysis of radiolabelled unmodified PrP resulted in a band at approximately 23 kDa representing a full-length translation product(Fig. 8, lane 1), as described previously [31]. This material was sensitive to digestion with 20 μg/ml PK (Fig. 8, lane 2). However, when PK digestion was carried out on radiolabelled unmodified translation products that had been incubated with unlabelled modified rPrP, the templated translation products acquired a PK-resistant core of 17–20 kDa (Fig. 8, lanes 3 and 4). As can be seen, a substantial fraction of the labelled protein was PK-resistant and is hence not degraded, giving rise instead to a strong band of protein of the size expected of the PK-resistant core. Each of these assays

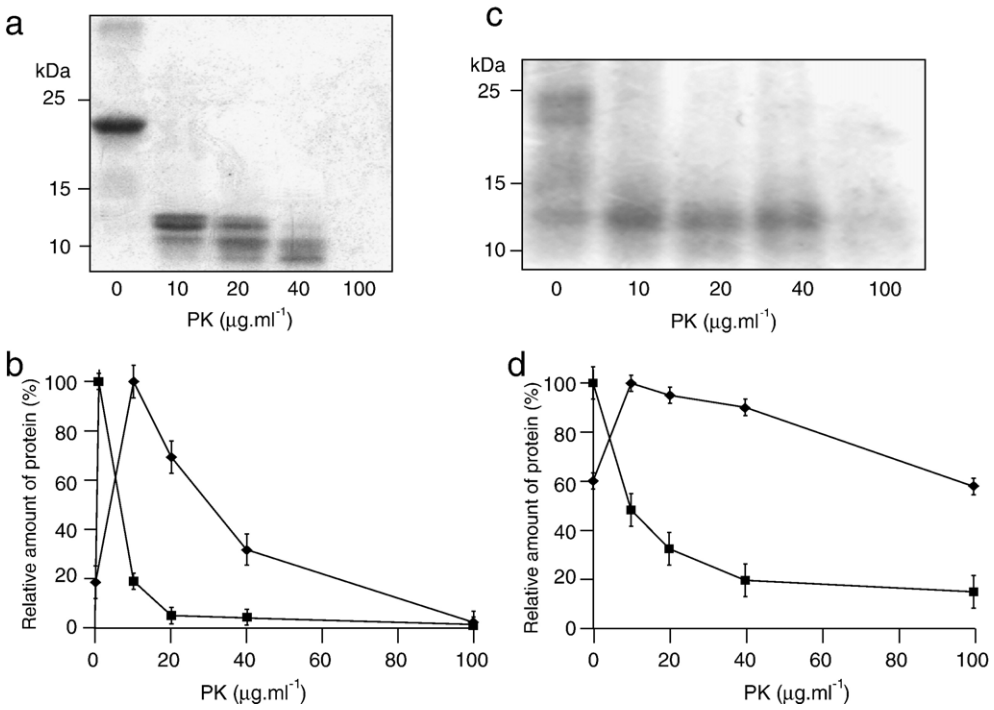

Fig. 5. Proteinase K resistance of modified rPrP. Unmodified (a and b) or modified (c and d) rPrP (1 mg/ml), was incubated with increasing concentrations of PK as described in Methods, and the samples analysed by Coomassie staining after SDS-PAGE (a and c). Densitometric analysis of SDS-PAGE (b and d) recorded changes in the level of protein species at 23 (filled square) and 12 kDa (filled diamond). ($n=3$ and Error bars depict one standard deviation). The 12-kDa fragment of modified protein showed a greater degree of PK resistance at levels of PK between 40 and 100μg/ml, as compared to unmodified protein.

would seem to indicate that both PK resistance and structure of the modified protein had been propagated onto unmodified rPrP.

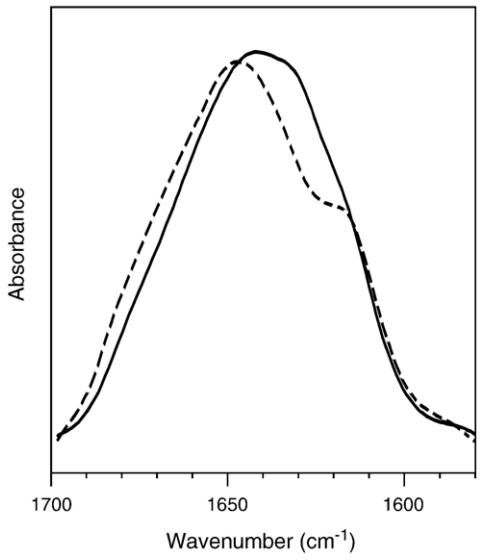

Fig. 6. Modified protein can propagate its structure onto unmodified protein. FT-IR spectra of unmodified rPrP (continuous line) and unmodified rPrP after it had been incubated with modified rPrP (dashed line), concentrations as in Methods. A shoulder at around 1620 cm^{-1} is evident in the templated unmodified protein indicative of the presence of β-sheet structures not present in the spectrum of the unmodified and untemplated protein.

4. Discussion

Two major pieces of evidence have supported the view that the difference between PrP^C and PrP^{Sc} resides in a change in secondary structure since the primary sequences of the two PrP isoforms are believed to remain identical and unmodified [42,14]. However, the presence of a population of chemically modified protein, whether minor or major, within the population of disease-associated PrP molecules that might act as an initiating template during PrP^C to PrP^{Sc} conversion has never been discounted [42]. It is important therefore, to establish whether modifications of amino acid residues within PrP protein may contribute to its conversion from PrP^C to PrP^{Sc} during disease pathogenesis. Identification of the biochemical pathways responsible for such modifications of PrP during prion diseases may prove to be suitable therapeutic targets for inhibiting or retarding the progression of these as yet invariably fatal conditions.

In our study reported here we have utilized the NO_2^-/H_2O_2 system used previously in studies on alpha-synuclein [25] to mimick oxidative stress-induced modification of rPrP. Mass spectrometric analysis of NO_2^-/H_2O_2 modified rPrP showed that several tyrosine residues within the protein had been nitrated in addition to oxidative modifications to other susceptible amino-acids. Interestingly, when a dilution series of NO_2^-/H_2O_2 reactants was tested, no nitration of rPrP amino acid residues, or corresponding change of secondary structure, occurred at concentrations of nitrite or peroxide lower than 10 mM as determined by western blotting and CD spectroscopy (see

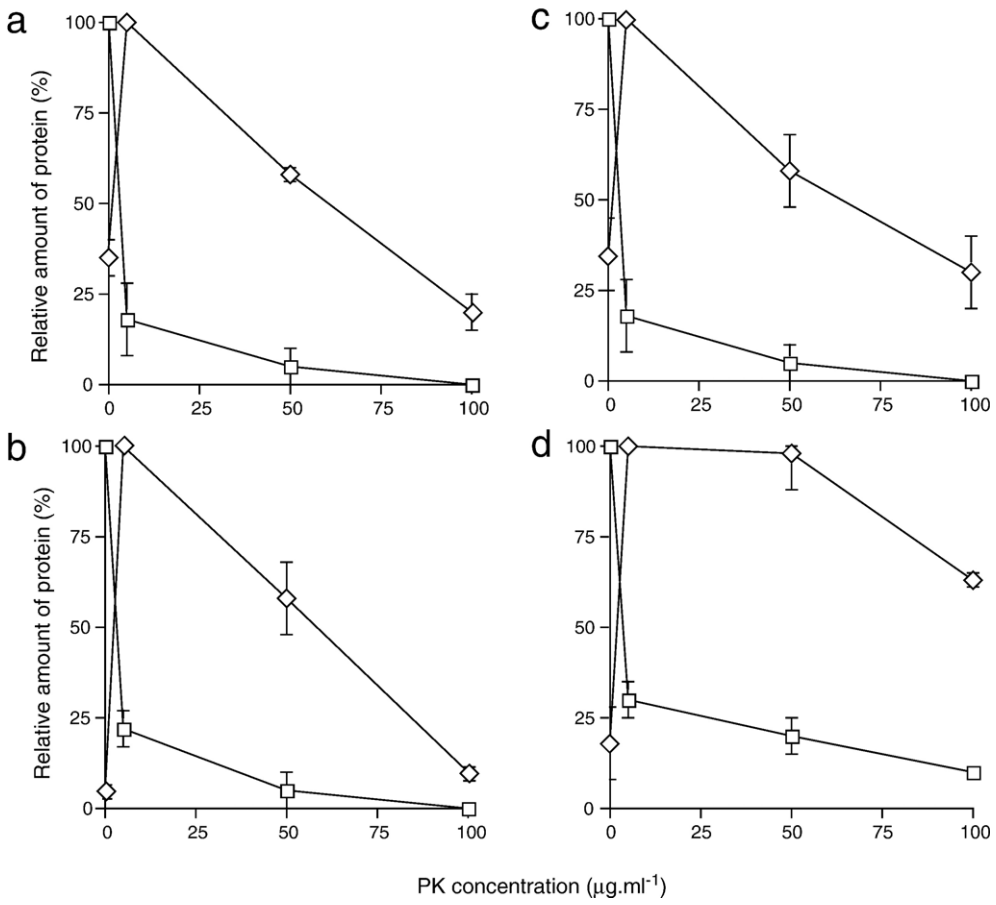

Fig. 7. Ability of modified rPrP to act as a template—using unlabelled rPrP. Unmodified rPrP was incubated in the absence (graphs a and c) or presence (graphs b and d) of modified rPrP for 0 (graphs a and b) or 24 h (graphs c and d), as described in Methods. After incubation, modified rPrP was removed by centrifugation, as described in Methods, and the supernatants of unmodified rPrP were treated with various concentrations of PK and analyzed by SDS-PAGE followed by Coomassie staining, as described in Methods. Densitometry recorded relative amount of protein present at approximately 23 kDa(open square) and 12 kDa (open diamond). Incubation in the presence of rPrP caused an increase in the amount of PK-resistant 12 kDa fragments. The results represent the mean of several independent samples from the same batch of protein. Error bars depict one standard deviation.

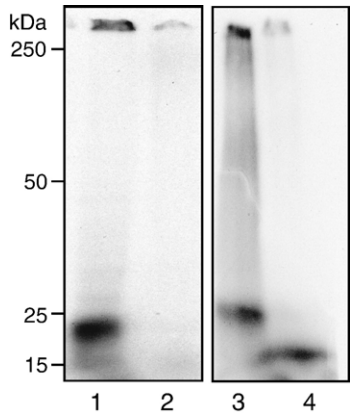

Fig. 8. Ability of modified rPrP to act as a template—using labelled rPrP. Modified rPrP can confer proteinase K resistance to unmodified rPrP, indicating that the modified protein can act as a template to unmodified rPrP. ^{35}S-labelled rPrP produced by *in vitro* translation was incubated for 16 h at 37 °C with unlabelled modified rPrP. Samples were analyzed by SDS-PAGE and autoradiography. Lane 1, unmodified rPrP produced by coupled in vitro transcription/translation product of the ovine PrP gene; lane 2, PK digest of unmodified rPrP translation product; lane 3, unmodified rPrP translation product templated with modified rPrP; lane 4, PK digest of templated unmodified rPrP translation product.

previously). This is similar to studies reported by others which have shown that it is only at high nitrite concentrations (around 1 mM or above) that MPO catalyzes tyrosine nitration [43]. At physiological levels of nitrite (0.5–210 μM) very little nitration of tyrosine residues occurs. Accordingly, tyrosine nitration may only be promoted in extracellular sites where nitric oxide fluxes are high and superoxide and hypochlorite levels are not sufficient to inhibit the reaction. However, the primary intention with this study was to achieve PTMs which might cause a conformational change. It is unlikely that the conditions used to achieve this might occur in vivo even at sites undergoing oxidative stress during prion disease. Moreover, as yet there is no report of nitrated PrP having been detected in infected material. However, it is still possible that a minor population of modified protein might not have been detected. This might be sufficient to allow propagation of conformational change even though the majority population of PrP^{Sc} studied would not contain any modification per se.

The kinetics of modified rPrP aggregation under the conditions used in our studies was that of an apparent first order reaction, dependent solely on the concentration of rPrP.

Previous studies have suggested that a constant rate of aggregate growth is indicative of a non-specific disordered process, as might be expected with rapid aggregate formation that occurs in a time scale of minutes rather than the more ordered process of fibrillization which occurs in a time scale of hours [44]. Furthermore, it has been predicted that amyloid fibrillogenesis of PrP is far more complex than disordered non-specific aggregation but instead, consists of several stages of nucleation and elongation each with their own distinct set of kinetic parameters [44–46]. The physical nature of PrP aggregates that occur in vivo during prion disease are either amorphous or amyloid, such as scrapie-associated fibrils (SAFs) [14]. The aggregates of modified rPrP reported here appeared to be a mixture of physical forms comprising predominately amorphous material inter-dispersed with fibrillar material. The observed fibrillar material was of similar dimensions and helical appearance to SAFs observed by electron microscopy following sucrose gradient fractionation of scrapie-infected hamster brains [47,48], but were unlike fibrils formed in more recent work using recombinant protein [49].

Modification of rPrP induced by the NO_2^-/H_2O_2 system resulted in significant structural changes within the protein as evidenced by FT-IR spectroscopy. FT-IR spectra of unmodified rPrP were characterised by a narrow amide I band centered at 1652 cm^{-1} indicative of α-helical structure. In contrast, spectra of modified rPrP was characterised by a broader amide I band centred at 1648 cm^{-1}, in addition to a well-defined component at 1621 cm^{-1}, which is characteristic of β-sheet structure. These data clearly indicated that the conformational change in rPrP following oxidation/nitration was an increase in β-sheet content with a simultaneous decrease in α-helix and random coil structure.

A further property of rPrP exposed to NO_2^-/H_2O_2 was the acquisition of PK resistance, a feature characteristic of PrP^{Sc}. Protease resistant aggregates of other proteins, such as lysozyme and immunoglobulin light chains, that have been exposed to high levels of oxidative stress reactants have also been observed [50,51]. This is believed to occur as a consequence of steric hindrance within the protein aggregate with the resultant loss of enzyme access to the proteolytic cleavage site. The PK resistance of modified rPrP observed in our study could be due to a similar phenomenon. Protease-resistance of the core of PrP has long been established as a key characteristic by which PrPC and PrPSc are distinguished [52–54]. Consequently, PK has been established as the proteolytic enzyme used in both preparative and diagnostic detection of PrPSc [47,55,56]. PK is an endolytic protease known to hydrolyse the peptide bond on the carboxylic side of aromatic, aliphatic or hydrophobic amino acid residues [57]. It is possible therefore, that the acquisition of PK resistance by NO_2^-/H_2O_2 exposed rPrP was a consequence not only of changes in protein secondary structure but also was the result of chemical modification of key amino acids within the protein molecule. This view is supported by the observations that show that di-tyrosine cross-linking, a chemical modification known to occur under conditions of OS, renders proteins resistant to proteolytic degradation [21]. In vivo, PK-resistant PrP^{Sc} is glycosylated and is generally characterised by a PK-resistant core migrating to between 27 and 30 kDa by SDS-PAGE [5]. Consequently unglycosyated PrP^{Sc} is expected to have a protease-resistant core of around 17 kDa [5]. The PK-resistant core evident in the unglycosylated modified rPrP in the experiments reported here was 12 kDa. This indicates that the our modifications of rPrP do not appear to have resulted in a conformational form of PrP that is completely analogous that found in vivo within TSE affected individuals. However, recent reports of a sub-population of PrP^{Sc} in sporadic CJD cases with a PK-resistant core of 12 kDa, indicate that our protein may have a structure similar to this protein. Interestingly, rPrP refolded into fibrils, analogous to those shown to be infectious [7] has also been shown to have limited PK-resistance and generates a PK-resistant core of similar size [49].

In future work, we need to assess the effects of oxidative stress reactants on glycosylated and membrane-bound/cellular PrP^c and to demonstrate their effect on cells in culture. This is especially the case in the light of recent work by the Aguzzi group [58] which shows that chronic inflammation can lead to an expanded and unexpected distribution of prions. As chronic inflammation is commonly associated with oxidative stress conditions, our findings of their effects on the conformation of recombinant prion protein may well reflect the reasons behind this expanded distribution. With respect to PK-resistance, it should be noted that parallel experiments on lysozyme also gave rise to a PK-resistant core. This indicated that the effect of modifying a protein and affecting its resistance to PK is not specific to prion protein. However, as sequence similarity is a prerequisite to templating ability [40] it is unlikely that modified lysozyme would act as a template for conversion of unmodified recombinant prion protein.

A key finding in our experiments was the observation that modified rPrP could act as a template to induce PrP^{Sc}-like characteristics in unmodified rPrP. In our study the templating ability was assessed by the induction of both structural modification and PK resistance as has been utilized in other *in vitro* conversion assay systems [40,59]. The fact that the modified rPrP aggregated and could be pelleted by centrifugation meant that this material could be separated from unmodified rPrP to allow a comparison of the secondary structures of the two forms of PrP. It should be noted that the FT-IR spectrum of the unmodified protein prior to templating had a broader alpha-helical peak than expected. This observed increase in beta sheet secondary structure detected on FT-IR analysis of stored unmodified rPrP as well as the increase in PK resistance of the 12-kDa digestion products of stored unmodified rPrP (see below) would seem to reinforce observations of others that spontaneous conformational changes might occur in stored recombinant protein due to spontaneous PTMs such as deamidation and/or oxidation [15]. Confirmation of this possibility will require future mass spectroscopic analysis of such stored protein samples. The FT-IR spectral analysis of unmodified, templated rPrP that remained in the supernatant of the templating reaction mixture gave a well-resolved β-sheet band which was absent in the untemplated sample and resembles the spectrum of the modified protein in Fig 3.

In addition to templating structural changes, modified rPrP was also capable of inducing PK-resistance in unmodified rPrP. Results from the radiolabelled protein translation templating experiment showed the presence of a 17-kDa PK-resistant PrP core of unmodified rPrP following incubation with modified rPrP whereas the digestion product was 12 kDa when recombinant PrP was used. The difference in size between the PK digestion products obtained in the two templating experiments could have been due to a number of factors which need to be resolved. The radiolabelled PrP translation product is unglycosylated and before incubation in the presence of modified rPrP is digested completely in the presence of PK. Unglycosylated PrPSc is expected to yield a product size of 17 kDa on PK digestion [40] and therefore, we could claim that as the radiolabelled translation product yields a 17-kDa product after templating, this product is of the expected size. However, the translation product was produced with the leader peptide in place and it is possible that this may not have been removed by the PK due to steric hindrance. This might account for the increased size of this digestion product in comparison to that obtained from the templating experiment using rPrP. Alternatively, the leader peptide may have been removed and the 17-kDa product could have resulted from the templating of an alternative conformation from the modified rPrP template, which was PK resistant. The 12-kDa digestion product which resulted from the experiment using modified rPrP as the template in the presence of excess unmodified rPrP is smaller than expected and would tend to suggest that our modifications have not produced a molecule entirely similar to PrPSc. Alternatively, it could be speculated that this is an, as yet, unidentified peculiarity of our rPrP. Collectively, our data support a view that PTMs within PrP can induce PrP^{Sc}-like characteristics within the protein and that these characteristics can be templated onto unmodified PrP. It is likely that other PTMs may induce PrP^{Sc}-like qualities in PrP. Our own unpublished data has shown that arginine to citrulline modifications of rPrP can also change the secondary structure of PrP and produce a 12-kDa PK-resistant core (Young et al., in preparation). Moreover, arginine to citrulline modifications have been found in PrP^{Sc} [60]. In addition, copper has been shown to induce the production of oxo-histidine and/or aspartate in rPrP that subsequently results in aggregation of the molecule [61]. It would seem pertinent to analyze further those PTMs and their combinations. that are capable of inducing both secondary structural changes and PK-resistance in rPrP that more closely resemble PrP^{Sc}-like characteristics displayed by disease-associated PrP found in vivo during prion disease, for example a 17-kDa unglycosylated PK-resistant core. Furthermore, identification of the biochemical pathways responsible for the modification induced by oxidative stress conditions on PrP may offer new targets for therapeutic intervention in prion diseases.

Acknowledgements

DVD was supported by the Department of Health. DSY held a BBSRC studentship. FM was supported by a Marie Curie Intra-European Fellowship within the 6th European Community Framework Programme. ACG, DO and JW would like to thank BBSRC for continued support. We thank Dr. Raymond Budjoso, Dr. Alana Thakray and Mr. Tim Fitzmaurice of the Veterinary School, University of Cambridge for their kind help in earlier preparations of the manuscript and Dr. Paul Dear for unending help and support.

References

[1] G.A.H. Wells, A.C. Scott, C.T. Johnson, R.F. Gunning, R.D. Hancock, M. Jeffrey, et al., A novel progressive spongiform encephalopathy in cattle, Vet. Rec. 121 (1987) 419–420.
[2] T.C. Britton, S. Al-Sarraj, C. Shaw, T. Campbell, J. Collinge, Sporadic Creutzfeldt–Jakob disease in a 16 year-old in the UK, Lancet 346 (1995) 1155.
[3] R.H. Kimberlin, Scrapie, Br. Vet. J. 137 (1981) 105–112.
[4] P.A. McBride, M.E. Bruce, H. Fraser, Immunostaining of cerebral amyloid plaques with antisera raised to scrapie-associated fibrils (SAF), Neuropathol. App. Neurobiol. 14 (1988) 325–336.
[5] S.B. Prusiner, Molecular biology of prion diseases, Science 252 (1991) 1515–1522.
[6] G.S. Jackson, L.L. Hosszu, A. Power, et al., Reversible conversion of monomeric human prion protein between native and fibrillogenic conformations, Science 283 (1999) 1935–1937.
[7] G. Legname, I.V. Baskakov, H.O. Nguyen, D. Riesner, F.E. Cohen, S.J. DeArmond, S.B. Prusiner, Synthetic mammalian prions, Science 305 (2004) 673–676.
[8] G. Legname, H.O. Nguyen, I.V. Baskakov, F.E. Cohen, S.J. Dearmond, S.B. Prusiner, Strain-specified characteristics of mouse synthetic prions, Proc. Natl. Sci. Acad. USA 102 (2005) 2168–2173.
[9] A. Tahiri-Alaoui, A.C. Gill, P. Disterer, W. James, Methionine 129 variant of human prion protein oligomerizes more rapidly than the valine 129 variant: implications for disease susceptibility to Creutzfeldt–Jakob disease, J. Biol. Chem. 279 (2004) 31390–31397.
[10] I.V. Baskakov, Legname, M.A. Baldwin, S.B. Prusiner, F.E. Cohen, Pathway complexity of prion protein assembly into amyloid, J. Biol. Chem. 277 (2004) 21140–21148.
[11] B.S. Wong, H. Wang, D.R. Brown, I.M. Jones, Selective oxidation of methionine residues in prion proteins, Biochem. Biophys. Res. Commun. 259 (1999) 352–355.
[12] H.E.M. McMahon, A. Mange, N. Nishida, C. Creminon, D. Casanova, S. Lehmann, Cleavage of the amino terminus of the prion protein by reactive oxygen species, J. Biol. Chem. 276 (2001) 2286–2291.
[13] J.R. Requena, M.N. Dimitrova, et al., Oxidation of methionine residues in the prion protein by hydrogen peroxide, Archiv. Biochem. Biophys. 432 (2004) 188–195.
[14] A.C. Gill, M.A. Ritchie, L.G. Hunt, S.E. Steane, K.G. Davies, S.P. Bocking, A.G. Rhie, A.D. Bennett, J. Hope, Post-translational hydroxylation at the N-terminus of the prion protein reveals presence of PPII structure in vitro, EMBO J. 19 (2000) 5324–5331.
[15] K. Qin, D.S. Yang, Y. Yang, M.A. Chishti, L.J. Meng, H.A. Kretzschmar, C.M. Yip, P.E. Fraser, D. Westaway, Copper(II)-induced conformational changes and protease resistance in recombinant and cellular PrP. Effect of protein age and deamidation, J. Biol. Chem. 275 (2000) 19121–19131.
[16] J.D. Wadsworth, A.F. Hill, S. Joiner, G.S. Jackson, A.R. Clarke, J. Collinge, Strain-specific prion-protein conformation determined by metal ions, Nat. Cell Biol. 1 (1999) 55–59.
[17] K.-M. Pan, M. Baldwin, J. Nguyen, et al., Conversion of alpha - helices into beta sheets features in the formation of scrapie prion proteins, Proc. Natl. Acad. Sci. USA 90 (1993) 10962–10966.
[18] N. Das, R.L. Levine, W.C. Orr, R.S. Sohal, Selectivity of protein oxidative damage during aging in *Drosophila melanogaster*, Biochem. J. 360 (2001) 209–216.
[19] M. Guentchev, T. Voigtlander, C. Haberler, M.H. Groschup, H. Budka, Evidence for oxidative stress in experimental prion disease, Neurobiol. Dis. 7 (2000) 270–275.

[20] Y.G. Choi, J.I. Kim, H.P. Lee, J.K. Jin, E.K. Choi, R.I. Carp, Y.S. Kim, Induction of heme oxygenase-1 in the brains of scrapie-infected mice, Neurosci. Lett. 289 (2000) 173–176.
[21] B. Van Everbroeck, I. Dobbeleir, M. De Waele, E. De Leenheir, U. Lubke, J.-J. Martin, P. Cras, Extracellular protein deposition correlates with glial activation and oxidative stress in Creutzfeldt–Jakob and Alzheimer's disease, Acta Neuropathol. 108 (2004) 194–200.
[22] B.S. Berlett, E.R. Stadtman, Protein oxidation in aging, disease, and oxidative stress, J. Biol. Chem. 272 (1997) 20313–20316.
[23] M. Hashimoto, A. Takeda, L.J. Hsu, T. Takenouchi, E. Masliah, Role of cytochrome *c* as a stimulator of alpha-synuclein aggregation in Lewy body disease, J. Biol. Chem. 274 (1999) 28849–28852.
[24] L. Galeazzi, P. Ronchi, C. Franeschi, S. Giunta, In vitro peroxidase oxidation induces stable dimers of beta amyloid (1–42) through dityrosine formation, Amyloid 1 (1999) 7–13.
[25] J.M. Souza, B.I. Giasson, Q. Chen, V.-M.Y. Lee, H. Ischiropoulos, Dityrosine cross-linking promotes formation of stable alpha-synuclein polymer, J. Biol. Chem. 275 (2000) 18344–18349.
[26] D.K. Choi, S. Pennathur, C. Perier, K. Tieu, P. Teismann, D.C. Wu, V. Jackson-Lewis, M. Vila, J.P. Vonsattel, J.W. Heinecke, S. Przedborski, Ablation of the inflammatory enzyme myeloperoxidase mitigates features of Parkinson's disease in mice, J. Neurosci. 25 (2005) 6594–6600.
[27] L.A. Macmillan-Crow, J.P. Crow, J.A. Thompson, Peroxynitrite-mediated inactivation of manganese superoxide dismutase involves nitration and oxidation of critical tyrosine residues, Biochemistry 37 (1998) 1613–1622.
[28] A. Rhie, L. Kirby, et al., Characterization of 2′-fluoro-RNA aptamers that bind preferentially to disease-associated conformations of prion protein and inhibit conversion, J. Biol. Chem. 278 (2003) 9697–9705.
[29] V. Cabiaux, R. Brasseur, R. Wattiez, P. Falmagne, J.-M. Ruysschaert, E. Goormaghtigh, Secondary structure of diphtheria toxin and its fragments interacting with acidic liposomes studied by polarized infrared spectroscopy, J. Biol. Chem. 264 (1989) 4928–4938.
[30] H. Puchtler, F. Sweat, M. Levine, Method of staining with Congo Red, J. Histochem. Cytochem. 10 (1962) 355–364.
[31] D.V. Dear, T.J. Fitzmaurice, P.J. Goymer, S.-J. Richards, Rapid expression of polymorphic ovine prion proteins and studies on their protease sensitivity, Brain Res. Bull. 48 (1999) 89–92.
[32] A. Van der Vliet, J.P. Eiserich, B. Halliwell, C.E. Cross, Formation of reactive nitrogen species during peroxidase-catalyzed oxidation of nitrite—A potential additional mechanism of NO-dependent toxicity, J. Biol. Chem. 272 (1997) 7617–7625.
[33] S. Pennathur, V. Jackson-Lewis, S. Przedborski, J.W. Heinecke, Mass spectrometric quantitation of 3-nitrotyrosine, ortho tyrosine and o,o′-dityrosine in brain tissue of 1-methyl-4-phenyl-1,2,3,6-tetrahydropyridine-treated mice—A model of oxidative stress in Parkinson's disease, J. Biol. Chem. 274 (1999) 34621–34628.
[34] H. Ischiropoulos, L. Zhu, J. Chen, H.M. Tsai, J.C. Martin, C.D. Smith, J.S. Beckman, Peroxynitrite-mediated tyrosine nitration catalyzed by superoxide dismutase, Arch. Biochem. Biophys. 298 (1992) 431–437.
[35] A. Bakhoj, N.H. Heegaard, Monitoring nitrotyrosinylation of asynthetic peptide by capillary zone electrophoresis, Electrophoresis 20 (1999) 2519–2523.
[36] R.T. Dean, S. Fu, R. Stocker, M.J. Davies, Biochemistry and pathology of radical-mediated protein oxidation, Biochem. J. 324 (1997) 1–18.
[37] M.P. Morrissey, E.I. Shakhnovich, Evidence for the role of PrPc helix 1 in the hydrophilic seeding of prion aggregation, Proc. Natl. Acad. Sci. U. S. A. 96 (1999) 11293–11298.
[38] R. Reik, S. Hornemann, G. Wider, M. Billeter, R. Glockshuber, K. Wutrich, NMR structure of the mouse prion protein domain PrP(121–321), Nature 382 (1996) 180–182.
[39] D.A. Lysek, C. Schorn, L.G. Nivon, V. Esteve-Moya, B. Christen, L. Calzolai, C. Von Schroetter, F. Fiorito, T. Herrmann, P. Guntert, K. Wutrich, Prion protein NMR structures of cats, dogs, pigs and sheep, Proc. Natl. Acad. Sci. U. S. A. 102 (2005) 640–645.
[40] G.J. Raymond, J. Hope, D.A. Kockisco, et al., Molecular assessment of the potential transmissibilities of BSE and scrapie to humans, Nature 388 (1997) 285–288.
[41] D.A. Kocisko, J.H. Come, S.A. Priola, B. Chesebro, G.J. Raymond, P.T. Lansbury, B. Caughey, Cell-free formation of protease-resistant prion protein, Nature 370 (1994) 471–474.
[42] N. Stahl, M.A. Baldwin, D.B. Teplow, L. Hood, B.W. Gibson, A.L. Burlingame, S.B. Prusiner, Structural studies of the scrapie prion protein using mass spectrometry and amino-acid sequencing, Biochemistry 32 (1993) 1991–2002.
[43] C.J. van Dalen, C.C. Winterbourn, R. Senthilmohan, A.J. Kettle, Nitrite as a substrate and inhibitor of myeloperoxidase, J. Biol. Chem. 275 (2000) 11638–11644.
[44] F. Chiti, P. Webster, N. Taddei, A. Clark, M. Stefani, G. Ramponi, C.M. Dobson, Designing conditions for in vitro formation of amyloid protofilaments and fibrils, Proc. Natl. Acad. Sci. U. S. A. 96 (1999) 3590–3594.
[45] A. Lomakin, D.S. Chung, G.B. Benedek, D.A. Kirschner, D.B. Teplow, On the nucleation and growth of amyloid beta-protein fibrils: detection of nuclei and quantitation of rate constants, Proc. Natl. Acad. Sci. U. S. A. 93 (1996) 1125–1129.
[46] M.M. Pallitto, R.M. Murphy, A mathematical model of the kinetics of β-amyloid fibril growth from the denatured state, Biophys. J. 81 (2001) 1805–1822.
[47] H. Diringer, H. Gelderblom, H. Hilmert, M. Ozel, R.H. Kimberlin, Scrapie infectivity, fibrils and low molecular weight protein, Nature 306 (1983) 476–478.
[48] H. Diringer, H. Hilmert, D. Simon, E. Werner, B. Ehlers, Towards purification of the scrapie agent, Eur. J. Biochem. 134 (1983) 555–560.
[49] O.V. Bocharova, L. Breydo, V.V. Salnikov, A.C. Gill, I.V. Baskakov, Synthetic prions generated *in vitro* are similar to a newly identified subpopulation of PrP^{Sc} from sporadic Creutzfeldt–Jakob disease, Prot. Sci. 14 (2005) 1222–1232.
[50] H.E. Jasin, Generation of IgG aggregates by the myeloperoxidase–hydrogen peroxide system, J. Immunol. 130 (1983) 1918–1923.
[51] E. Franzini, H. Sellak, J. Hakim, C. Pasquier, Oxidative damage to lysozyme by the hydroxyl radical: comparative effects of scavengers, Biochim. Biophys. Acta 1203 (1993) 11–17.
[52] D.C. Bolton, M.P. McKinley, S.B. Prusiner, Identification of a protein that purifies with the scrapie prion, Science 218 (1982) 1309–1311.
[53] S.B. Prusiner, Prions, Sci. Am. 251 (1984) 50–59.
[54] R.K. Meyer, M.P. McKinley, K.A. Bowman, M.B. Brownfield, R.A. Barry, S.B. Prusiner, Separation and properties of cellular and scrapie prion proteins, Proc. Natl. Acad. Sci. 83 (1986) 2310–2314.
[55] S.B. Prusiner, D.C. Bolton, D.F. Groth, K.A. Bowman, S.P. Cochran, M.P. McKinley, Further purification and characterisation of scrapie prions, Biochemistry 21 (1982) 6942–6950.
[56] W.A. Cooley, J.K. Clark, M.J. Stack, Comparison of scrapie-associated fibril detection and western immunoblotting for the diagnosis of natural scrapie, J. Comp. Pathol. 18 (1998) 41–49.
[57] W. Ebeling, N. Hennrich, M. Klockow, H. Metz, H.D. Orth, H. Long, Proteinase K from Tritirichim album Limber, Eur. J. Biochem. 47 (1974) 91–97.
[58] H. Seeger, M. Heikenwalder, et al., Coincident scrapie infection and nephritis lead to urinary prion excretion, Science 310 (2005) 324–326.
[59] L. Kirby, C.R. Birkett, K.H. Rudy, I.H. Gilbert, J. Hope, In vitro cell-free conversion of bacterial recombinant PrP to PrPres as a model for conversion, J Gen. Virol. 84 (2003) 1013–1020.
[60] J. Hope, G. Multhaup, L.J. Reekie, R.H. Kimberlin, K. Beyreuther, Molecular pathology of scrapie-associated fibril protein (PrP) in mouse brain affected by the ME7 strain of scrapie, Eur. J. Biochem. 172 (1988) 271–277.
[61] J.R. Requena, D. Groth, G. Legname, E.R. Stadtman, S.B. Prusiner, R.L. Levine, Copper-catalyzed oxidation of the recombinant SHa(29–231) prion protein, Proc. Natl. Acad. Sci. U. S. A. 98 (2001) 5–7178.